Entire Domain Basis Function with Accurate Edge Condition for Rectangular Microstrip Antennas

Raul O. Ribeiro, Marcos V. T. Heckler, *Member, IEEE,* and Alexis F. Tinoco-S.

Abstract—This letter presents the study of a segmented entire domain basis function suitable for fast analysis of rectangular microstrip antennas with the method of moments (MoM). In contrast to other basis functions, whereby the edge condition is valid only for narrow lines, the proposed basis function can be applied to microstrip lines and antennas with arbitrary width. For validation, a probe-fed rectangular microstrip antenna was modeled and the results were validated with measurements. The deviation of the calculated resonance frequency from the measured value could be reduced to less than 0.1%. This has been obtained with the use of only two expansion modes along each direction for the construction of the MoM matrices.

Index Terms—Basis functions, microstrip antennas.

I. INTRODUCTION

The analysis and optimization of large microstrip arrays and reflectarrays require fast methods to determine accurately input impedance, mutual coupling and radiation pattern. Approximate models, such as the transmission line method or the cavity model, are applicable only to microstrip antennas printed on thin substrates. This limitation can be overcome by using full-wave techniques, such as the finite element method (FEM) and the method of moments (MoM). The first technique is very flexible, but demands very large computational resources for the analysis of large structures. For large arrays, MoM can be a good option, if proper entire domain basis fucntions are used.

Among many other papers found in the literature, classical formulations of MoM are presented in [1] and [2]. In [1], the MoM is applied for the analysis of probe-fed antennas with rectangular and nonrectangular shapes. In [2], the calculation of input impedance and mutual coupling between rectangular patches is performed by using basis functions with sinusoidal behavior along the resonance without any variation of the current density in the orthogonal direction. In [3], an edge condition, which stands for the abrupt increase of the current density near the nonradiating edges of a rectangular patch, is introduced into the basis function, which yielded accurate results only for narrow lines with widths up to two times the substrate thickness. In [4], the edge condition proposed by [3] was initially included in the MoM modelling, but no improvement in the accuracy of the results in comparison to

R. O. Ribeiro is with the Department of Mathematics, Universidade Federal do Rio Grande do Sul, Porto Alegre, Brazil, e-mail: raul.oliveira.ribeiro@gmail.com.

M. V. T. Heckler is with Universidade Federal do Pampa, Alegrete, Brazil, e-mail: marcos.heckler@unipampa.edu.br.

A. R. Tinoco-S. is with Universidad de las Fuerzas Armadas (ESPE), Quito, Ecuador, e-mail: aftinoco@espe.edu.ec.

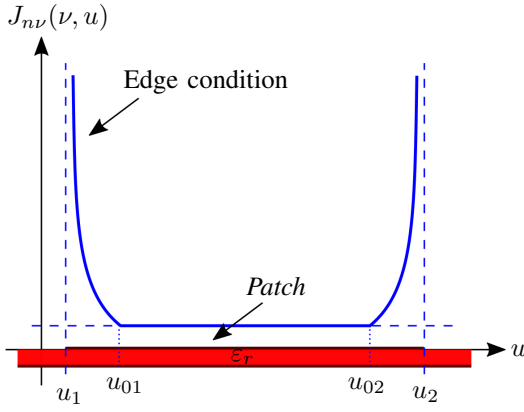Manuscript received October 20, 2017; revised...

simple sinusoidal basis fucntion has been verified. In [5]– [8], an edge condition was considered along with piecewise sinusoidal basis functions to model microstrip circuits on cylindrical substrates. Validation of this approach was achieved only for very thin substrates or narrow conducting strips.

In a more recent work, the basis functions are chosen for caracterization of reflectarrays composed of rectangular patches and crossed microstrip dipoles [9]. The authors used the basis function described in [10], [11], which yielded good results for substrate thicknesses greater than 0.04λ, where λ is the wavelength in the dielectric used for the reflectarray.

The edge condition considered in [3], [5]– [6] and [10] shows a continuous growth of the current density from the center of the patch to the edges in the direction orthogonal to the current flow. This formulation is valid only for narrow lines and is not efficient for wide microstrip lines and antennas. For this reason, this letter demonstrates the use of entire domain segmented basis functions to allow a more accurate representation of the edge condition. In the next section, the mathematical formulation for the proposed basis function is presented. Then, the performance of the proposed basis function is validated by comparison of results with [2], [10] and measured results. By using only two expansion modes along x and y to fill the MoM matrix, excellent agreement with experimental data has been achieved.

II. SEGMENTED BASIS FUNCTION

For the case of microtrip structures, the MoM is used to solve the electric field integral equation of the form [12]

$$\iint_S G\left(x, x', y, y'\right) \vec{J}_s\left(x', y'\right) dS = -\vec{E}^i\left(x, y\right), \quad (1)$$

where G is the Green's function of the layered structure, $\vec{J}_s$ is the unknown surface current density induced on the metalizations (patch or microstrip lines), and $\vec{E}^i$ is the incident electric field, which stands for the excitation of the structure. In the MoM formulation, $\vec{J}_s$ must be expanded in the form [13]

$$\vec{J}_s\left(x', y'\right) = \sum_{n=1}^{N_x} a_n J_{nx}\left(x', y'\right) \hat{x} + \sum_{n=1}^{N_y} b_n J_{ny}\left(x', y'\right) \hat{y}, \quad (2)$$

where J_{nx} and J_{ny} are known basis functions used to describe the surface current density $\vec{J}_s$ along the x and y-directions, respectively, and a_n and b_n are the coefficients to be determined. It is well known that the number of needed terms N_x and N_y for the expansion depends strongly on how good the basis functions can represent the behaviour of $\vec{J}_s$.

Standard entire domain basis functions need the use of several modes to represent accurately the current distribution

Fig. 1: Representation of the segmented edge condition along the direction orthogonal to the current flow.

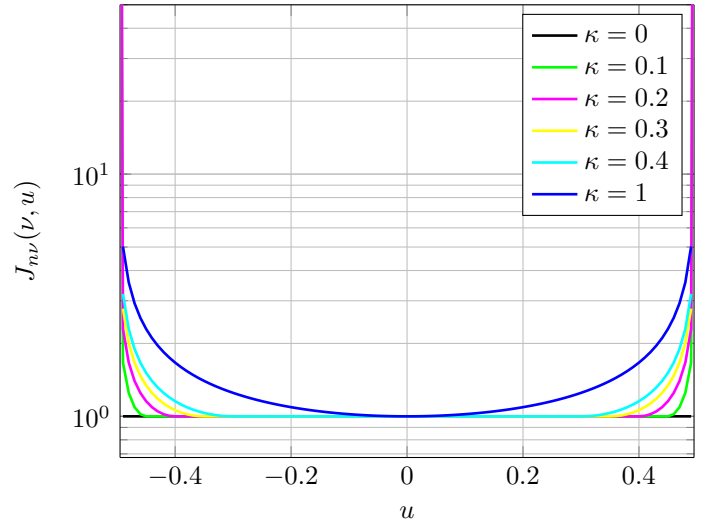Fig. 2: Transverse behaviour of the segmented basis function for different values of κ.

Fig. 3: Geometry of a probe-fed rectangular microstrip antenna.

on the patch surface. The main consequence is the increase of the MoM matrix, hence resulting in larger memory usage and computation time. These disadvantages can be overcome by defining an entire domain basis function with segmented representation, whereby the flat behaviour near the center and an abrupt increase near the edges can be controlled properly. This behavior is graphically depicted in Fig. 1, where ν stands for the direction of current flow and u is the coordinate orthogonal to ν. The basis function proposed in this letter presents sinusoidal behavior in the ν-direction, whereas the variation along u can be described as

$$h(u) = \begin{cases} \left[1 - \left(\frac{u-u_{01}}{u_b}\right)^2\right]^{-1/2} & \text{for } u_1 < u < u_{01} \\ 1 & \text{for } u_{01} < u < u_{02} \\ \left[1 - \left(\frac{u-u_{02}}{u_b}\right)^2\right]^{-1/2} & \text{for } u_{02} < u < u_2 \end{cases}, \quad (3)$$

where $u_b = \kappa \frac{|u_2 - u_1|}{2}$, $u_{01} = u_1 + u_b$ and $u_{02} = u_2 - u_b$. In this approach, the function is divided into three parts, whereby the edge condition can be easily applied to a narrow region close to the patch edges, in contrast to previous formulations found in the literature. The patch width is given by $|u_2 - u_1|$ and the edge condition is applied between the points u_1 and u_{01}, and u_{02} and u_2. The parameter κ can be used to choose how close to the edges the segmentation should take place. The range of possible values is $0 \leq \kappa \leq 1$, whereby $\kappa = 0$ stands for the case without edge condition, as defined in [2], and $\kappa = 1$ is the case without segmentation, which is the case analyzed in [10]. In Fig. 2, the behavior along the u-direction is plotted for different values of κ.

By using this mathematical formulation, the basis function for a rectangular patch is described by (4) and (5) in the space domain along x and y, respectively, as given in Appendix A. In the spectral domain, the functions assume the form given by (6) and (7) in Appendix B.

III. VALIDATION

For the validation of the proposed basis function, a probe-fed singly-layered rectangular microstrip antenna was designed to resonate at 2.35 GHz and manufactured according to the geometry sketched in Fig. 3. The antenna dimensions and the electrical parameters of the substrate are summarized in Table I. The fabricated prototype is shown in Fig. 4.

The MoM was implemented considering the Galerkin approach and the Green's function for singly layered antennas as described in [11], [14], [15]. Considering that the current density on the patch flows primarily along the y direction, the MoM computations were run including only the expansion modes $n = 1$ and $n = 2$ along x, and $n = 1$ and $n = 3$ along y. The performance of the proposed basis function in comparison to [2], [10] and measured results is demonstrated

TABLE I: Microstrip antenna dimensions and electrical parameters.

Parameter	Value
Patch length (L)	42.21 mm
Patch width (W)	33.79 mm
Substrate thickness (h)	1.524 mm
Dielectric constant (ε_r)	3.38
Loss tangent ($tan\delta$)	0.0034
Feed position (x_p, y_p)	$(0, -6.2\ mm)$

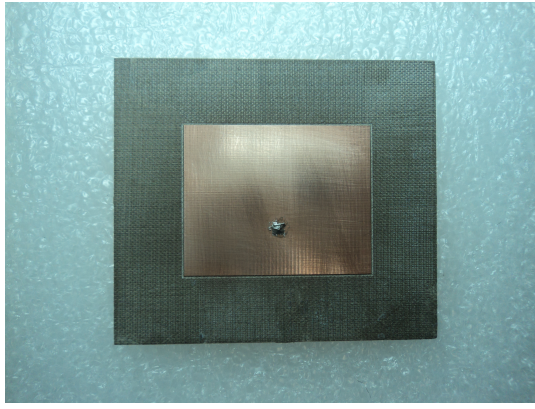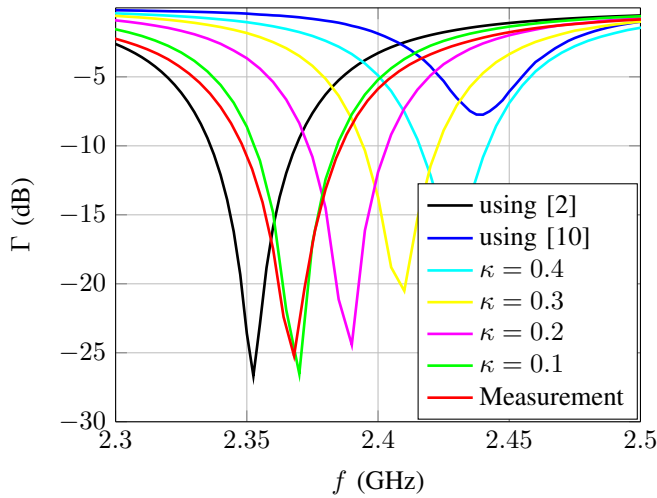Fig. 4: Top view of the prototype.

Fig. 5: Comparison of reflection coefficient curves for different basis functions and measured results.
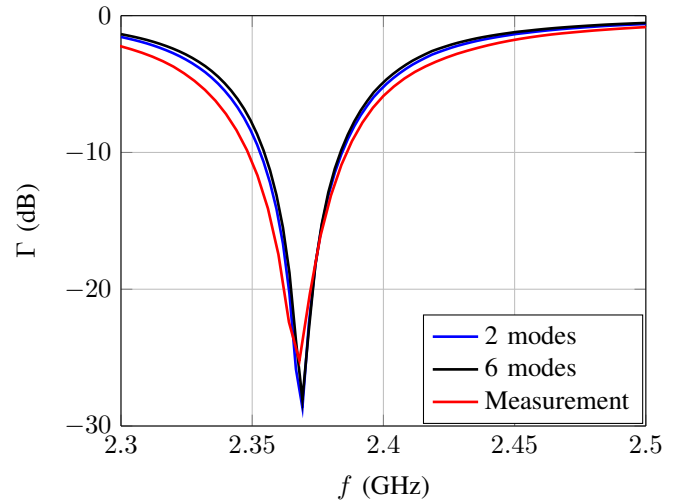

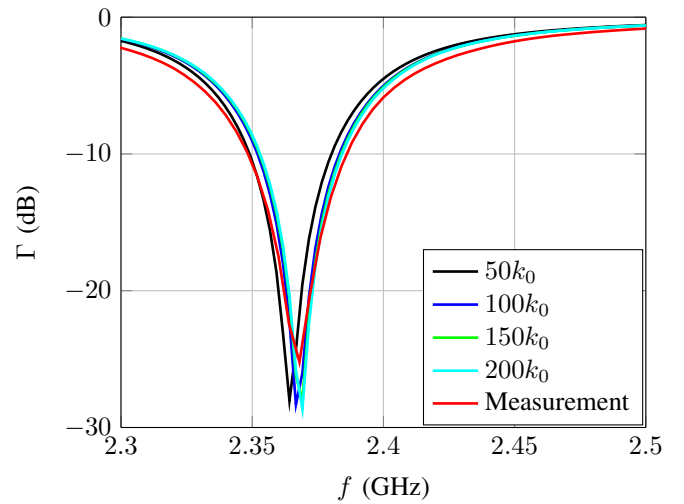Fig. 6: Variation of the reflection coefficient for different numbers of expansion modes.

Fig. 7: Variation of the reflection coefficient for different stopping criteria for the integration of the inverse Fourier transform.

in Fig. 5. Very good agreement has been obtained with measurements by setting $\kappa = 0.1$. In terms of resonance frequency, the value obtained with the measured curve was 2.368 GHz, whereas for $\kappa = 0.1$ it was 2.37 GHz. This means a deaviation of less than 0.1% from the measured result. The basis function of [10] yielded the largest frequency shift among the calculated cases. It should be pointed out that the design resonance frequency (2.35 GHz) is located at the lower border of the operating band of the prototype, if the definition of bandwidth is taken as reflection coefficient lower than -10 dB. Although the optimum value for κ may vary according to the width of the patch, generally small values must be set, since the abrupt current growth occurs only very close to the non-radiating edges of the antenna. If W becomes much narrower than L, then κ must be increased. As demonstrated in [9], [10], for very narrow structures, such as transmission lines in microstrip or stripline technology, accurate results can be obtained by setting $\kappa = 1$.

The convergence of the solution has been tested for different number of modes used to expand the current on the patch and in terms of stopping criterion for the integration needed for the inverse Fourier transforms. The results for both analyses by considering κ=0.1 are shown in Figs. 6 and 7. The curves show that the increase in the number of modes beyond two does not present strong influence on the results, since the inclusion of the edge condition in the proposed basis function contributes to the precise description of the current induced on the patch. Additionally, the integration for the inverse Fourier transform can be stopped after $\beta = 150k_0$ without great impact on the accuracy.

The current distribution obtained with the MoM computation by setting $\kappa = 0.1$ is shown in Fig. 8. By analyzing the behavior of J_y, the expansion mode for $n = 1$ predominates along the y-direction, where the typical surface current distribution shape with the edge condition can be clearly identified [12].

IV. CONCLUSION

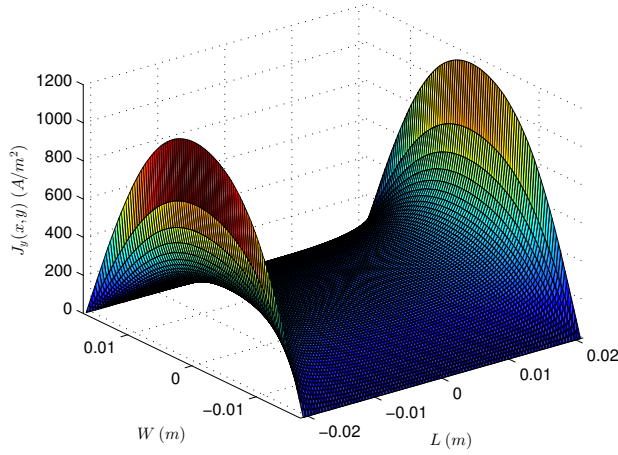In this letter, a basis function to take the edge condition accurately into account was proposed. The model presented

Fig. 8: Current distribution in the y-direction (J_y) obtained using basis functions with segmented edge condition and $\kappa = 0.1$.

very accurate representation of the surface current distribution for rectangular patch antennas. Due to the efficient modelling of the edge condition, only 2 expansion modes along x and y were needed to achieve accurate results. The proposed basis function should allow fast analysis of rectangular microstrip antennas, which is an interesting feature for many applications, such as the design of reflectarrays, whereby optimization of the radiation pattern is done iteratively by means of running MoM computations repeatedly.

APPENDIX A
SPACE DOMAIN BASIS FUNCTIONS

Entire domain basis functions for rectangular resonant patch, along the x and y-directions, are written in the space domain as

$$
J_{nx}(x,y) = \begin{cases}
\left[1 - \left(\frac{y-y_{01}}{y_b}\right)^2\right]^{-1/2} \sin\left(\frac{n\pi}{L}(x - L/2)\right) \\
\quad \text{for} \quad \begin{aligned} -L/2 &< x < L/2 \\ y_1 &< y < y_{01} \end{aligned} \\[2ex]
\sin\left(\frac{n\pi}{L}(x - L/2)\right) \\
\quad \text{for} \quad \begin{aligned} -L/2 &< x < L/2 \\ y_{01} &< y < y_{02} \end{aligned} \\[2ex]
\left[1 - \left(\frac{y-y_{02}}{y_b}\right)^2\right]^{-1/2} \sin\left(\frac{n\pi}{L}(x - L/2)\right) \\
\quad \text{for} \quad \begin{aligned} -L/2 &< x < L/2 \\ y_{02} &< y < y_2 \end{aligned}
\end{cases}
\tag{4}
$$

$$
J_{ny}(x,y) = \begin{cases}
\left[1 - \left(\frac{x-x_{01}}{x_b}\right)^2\right]^{-1/2} \sin\left(\frac{n\pi}{W}(y - W/2)\right) \\
\quad \text{for} \quad \begin{aligned} x_1 &< x < x_{01} \\ -W/2 &< y < W/2 \end{aligned} \\[2ex]
\sin\left(\frac{n\pi}{W}(y - W/2)\right) \\
\quad \text{for} \quad \begin{aligned} x_{01} &< x < x_{02} \\ -W/2 &< y < W/2 \end{aligned} \\[2ex]
\left[1 - \left(\frac{x-x_{02}}{x_b}\right)^2\right]^{-1/2} \sin\left(\frac{n\pi}{W}(y - W/2)\right) \\
\quad \text{for} \quad \begin{aligned} x_{02} &< x < x_2 \\ -W/2 &< y < W/2 \end{aligned}
\end{cases}
\tag{5}
$$

where n represents the mode of expansion, and $y_b = \kappa W/2$, $y_1 = -W/2$, $y_2 = W/2$, $y_{01} = W/2(-1+\kappa)$, $y_{02} = W/2(1-\kappa)$, $x_b = \kappa L/2$, $x_1 = -L/2$, $x_2 = L/2$, $x_{01} = L/2(-1+\kappa)$, $x_{02} = L/2(1-\kappa)$.

APPENDIX B
SPECTRAL DOMAIN BASIS FUNCTIONS

Applying the double Fourier transform defined in [12] to (4) and (5), the basis functions are written in the spectral domain as

$$
\tilde{J}_{nx}(k_x, k_y) = \left[\kappa\pi W J_0\left(\frac{1}{2}(1-\kappa)Wk_y\right)\right.
$$
$$
\left. + (1-\kappa)W \operatorname{sinc}\left(\frac{1}{2}(1-\kappa)Wk_y\right)\right]
$$
$$
\times \frac{\frac{n\pi}{L}}{k_x^2 - \left(\frac{n\pi}{L}\right)^2}\left[e^{-\frac{1}{2}jk_x L} - \cos(n\pi)e^{\frac{1}{2}jk_x L}\right]
\tag{6}
$$

$$
\tilde{J}_{ny}(k_x, k_y) = \left[\kappa\pi L J_0\left(\frac{1}{2}(1-\kappa)Lk_x\right)\right.
$$
$$
\left. + (1-\kappa)L \operatorname{sinc}\left(\frac{1}{2}(1-\kappa)Lk_x\right)\right]
$$
$$
\times \frac{\frac{n\pi}{W}}{k_y^2 - \left(\frac{n\pi}{W}\right)^2}\left[e^{-\frac{1}{2}jk_y W} - \cos(n\pi)e^{\frac{1}{2}jk_y W}\right]
\tag{7}
$$

where J_0 is Bessel function of the first kind and order zero.

REFERENCES

[1] E. Newman and P. Tulyathan, "Analysis of microstrip antennas using moment methods," *IEEE Transactions on Antennas and Propagation*, vol. 29, no. 1, pp. 47–53, Jan 1981.
[2] D. Pozar, "Input impedance and mutual coupling of rectangular microstrip antennas," *IEEE Transactions on Antennas and Propagation*, vol. 30, no. 6, pp. 1191–1196, Nov 1982.

[3] R. W. Jackson and D. M. Pozar, "Full-wave analysis of microstrip open-end and gap discontinuities," *IEEE Transactions on Microwave Theory and Techniques*, vol. 33, no. 10, pp. 1036–1042, Oct 1985.

[4] D. Pozar and S. Voda, "A rigorous analysis of a microstripline fed patch antenna," *IEEE Transactions on Antennas and Propagation*, vol. 35, no. 12, pp. 1343–1350, Dec 1987.

[5] R. Florencio, R. R. Boix, and J. A. Encinar, "Enhanced mom analysis of the scattering by periodic strip gratings in multilayered substrates," *IEEE Transactions on Antennas and Propagation*, vol. 61, no. 10, pp. 5088–5099, Oct. 2013.

[6] A. Nakatani and N. Alexopoulos, "Modeling microstrip circuits and microstrip antennas on cylindrical substrates," in *1986 Antennas and Propagation Society International Symposium*, vol. 24, Jun 1986, pp. 439–442.

[7] M. V. T. Heckler and A. Dreher, "Fast analysis of flush-mounted cylindrical microstrip structures," in *7th European Conference on Antennas and Propagation*, Apr. 2013, pp. 595–599.

[8] A. Nakatani and N. G. Alexopoulos, "Microstrip circuit elements on cylindrical substrates," in *1987 IEEE MTT-S International Microwave Symposium Digest*, vol. 2, May 1987, pp. 739–742.

[9] S. R. Rengarajan, "Choice of basis functions for accurate characterization of infinite array of microstrip reflectarray elements," *IEEE Antennas and Wireless Propagation Letters*, vol. 4, pp. 47–50, 2005.

[10] T. Itoh and W. Menzel, "A full-wave analysis method for open microstrip structures," *IEEE Transactions on Antennas and Propagation*, vol. 29, no. 1, pp. 63–68, Jan 1981.

[11] T. Itoh, *Numerical techniques for microwave and millimeter-wave passive structures*. Wiley-Interscience, 1989.

[12] R. Garg, P. Bhartia, I. Bahal, and A. Ittipiboon, *Microstrip Antenna Design Handbook*. Artech House, 2001.

[13] C. A. Balanis, *Antenna Theory: Analysis and Design, 2nd Ed.* John Wiley & Sons, 1997.

[14] Y. Ye, J. Yuan, and K. Su, "A volume-surface integral equation solver for radiation from microstrip antenna on anisotropic substrate," *International Journal of Antennas and Propagation*, vol. 2012, 2012.

[15] D. Pozar, "Radiation and scattering from a microstrip patch on a uniaxial substrate," *IEEE Transactions on Antennas and Propagation*, vol. 35, no. 6, pp. 613–621, Jun 1987.